Published in final edited form as:
Biochim Biophys Acta. 2018 January ; 1862(1): 61–70. doi:10.1016/j.bbagen.2017.10.006.

An increased autophagic flux contributes to the anti-inflammatory potential of urolithin A in macrophages

Yaw Duah Boakye[1], **Laura Groyer**, and **Elke H. Heiss**[*]
Department of Pharmacognosy, University of Vienna, Althanstrasse 14, 1090 Vienna, Austria

Abstract

Background—An extract of *Phyllanthus muellerianus* and its constituent geraniin have been reported to exert anti-inflammatory activity *in vivo*. However, orally consumed geraniin, an ellagitannin, shows low bioavailability and undergoes metabolization to urolithins by gut microbiota. This study aimed at comparing geraniin and urolithin A with respect to inhibition of M1 (LPS) polarization of murine J774.1 macrophages and shedding more light on possible underlying mechanisms.

Methods—Photometric, fluorimetric as well as luminescence-based assays monitored production of reactive oxygen species (ROS) and nitric oxide (NO), cell viability or reporter gene expression. Western blot analyses and confocal microscopy showed abundance and localization of target proteins, respectively.

Results—Urolithin A is a stronger inhibitor of M1 (LPS) macrophage polarization (production of NO, ROS and pro-inflammatory proteins) than geraniin. Urolithin A leads to an elevated autophagic flux in macrophages. Inhibition of autophagy in M1 (LPS) macrophages overcomes the suppressed nuclear translocation of p65 (NF-kB; nuclear factor kB), the reduced expression of pro-inflammatory genes as well as the diminished NO production brought about by urolithin A. The increased autophagic flux is furthermore associated with impaired Akt/mTOR (mammalian target of rapamycin) signaling in urolithin A-treated macrophages.

Conclusions and general significance—Intestinal metabolization may boost the potential health benefit of widely consumed dietary ellagitannins, as suggested by side by side comparison of geraniin and urolithin A in M1(LPS) macrophages. Increased activity of the autophagic cellular recycling machinery aids the anti-inflammatory bioactivity of urolithin A.

Keywords

Geraniin; Urolithin A; Macrophages; M1 polarization; Autophagy; mTOR

[*]Corresponding author. elke.heiss@univie.ac.at (E.H. Heiss).
[1]Current address: Department of Pharmaceutics, Kwame Nkrumah University of Science and Technology, Kumasi, Ghana.

Transparency document
The Transparency document associated with this article can be found, in online version.

1 Introduction

Phyllanthus muellerianus belongs to the family Euphorbiaceae, and leaves, bark and fruits are used in Traditional African Medicine for the treatment of dysentry, wounds and inflammatory disorders, among others [1]. Our recent study confirmed anti-inflammatory activity of an orally administered aqueous *Phyllanthus* leaf extract in rats and assigned part of its activity to its constituent geraniin [2]. Geraniin is an ellagitannin made up of a galloyl, a hexahydrodiphenoyl and a dehydrohexahydrodiphenoyl group esterified to a glucose molecule, most prominently present in different plant parts (leaf, root, seed, fruit) of the genera Euphorbiaceae, Geraniaceae and Phyllanthaceae [3]. Ellagitannins are generally very poorly absorbed from the gastrointestinal tract, possibly due to their bulky structure which does not facilitate simple diffusion. Therefore, metabolization of geraniin by intestinal microflora into ellagic acid, gallic acid, urolithin A, B and C and other related compounds is crucial for absorption [4,5]. Several bioactivities were assigned to geraniin, including improved wound healing [6], antiviral [7–9], growth inhibitory [10,11], hepato-, neuro-and cytoprotective [12–16] as well as anti-inflammatory [17] properties. However, given the low bioavailability and metabolization of geraniin it is questionable whether mere *in vitro* data may become relevant in an *in vivo* setting or whether the active principle beyond the observation made upon oral administration of geraniin is mainly the parent ellagitannin. In this line, it is of note that the reported bioactivities of urolithins partly overlap with those of geraniin, such as growth inhibition and anti-inflammation [18–22].

Inflammation represents a response to tissue injury induced by a multitude of stimuli, including wounds, infection, or transformed cells. Macrophages are crucial players in inflammation and show a high degree of phenotypic plasticity [23]. A simplistic classification divides macrophages in the classically activated M1 and the alternatively activated M2 types. However, this categorization only takes into account the extremes of a continuous spectrum macrophage states. M1 polarization usually results from of bacterial / Toll like receptor activation (*e.g.* by lipopolysaccharide (LPS)) and the presence of cytokines associated with a Th1-like response (*e.g.* interferon gamma (IFN-γ)). M1 macrophages produce pro-inflammatory cytokines and mediators (interleukin (IL)-12, IL-6, IL-1β, tumor necrosis factor (TNF)-α, reactive oxygen species (ROS) and reactive nitrogen species produced by inducible NO synthase (iNOS) or eicosanoids). In contrast, M2 polarization occurs upon exposure to cytokines connected with Th2 responses (such as IL-4 or IL-13). These cells are considered anti-inflammatory, produce IL-10 and highly express arginase 1 as well as scavenger receptors [24–26]. Despite being a vital defense reaction in the acute setting, ongoing chronic inflammation and production of cytokines and other pro-inflammatory factors can lead to tissue damage and is associated with chronic diseases, such as inflammatory bowel disease, the metabolic syndrome or declining cognitive function [27,28]. Therefore, compounds able to prevent or alleviate M1 polarization or boost the M1 → M2 shift may be promising candidates for countering those disorders and understanding their mode of action may even open up new therapeutic and intervention strategies.

Prompted by the results from our previous *in vivo* study with geraniin and from observations that ellagitannin-rich diets appear beneficial for patients with *e.g.* intestinal inflammation [29,30], we aimed in this study at comparing geraniin and the selected metabolite urolithin

A side-by-side in their impact on M1 macrophage polarization and revealing the potential underlying anti-inflammatory mechanism.

2 Material and methods

2.1 Chemicals and antibodies

Geraniin (purity ≥ 95%) was isolated and purified from leaves of *Phyllanthus muellerianus* [2]. Urolithin A (purity ≥ 98%) was obtained from Santa Cruz (Germany) and dihydrodichlorofluorescein-diacetate (H_2DCF-DA) from Invitrogen (Austria). All other chemicals or enzymes were obtained from Sigma-Aldrich (Austria). All primary and secondary antibodies were obtained from New England Biolabs (Germany), except the anti-iNOS and the anti-p65 antibodies from Santa Cruz (Germany), the anti-caspase1 antibody from Abcam (UK), the anti HO-1 antibody from Enzo Life Sciences (Germany) and the FITC-coupled anti-rabbit antibody from Sigma-Aldrich (Austria).

2.2 Cell culture

The J774.1 murine macrophage and the human embryonic kidney HEK (human embryonic kidney) 293 cell lines were obtained from ATCC (USA), and the stably transfected CHO (Chinese hamster ovary)-ARE-LUC reporter line was previously established in the lab [31]. All three cell lines were maintained in DMEM medium (phenol-red free; Lonza, Switzerland) supplemented with 10% fetal calf serum (Gibco, Germany), 2 mM glutamine (Lonza, Switzerland), 100 U/mL benzylpenicillin (Lonza, Switzerland), 100 μg/mL streptomycin (Lonza, Switzerland) at 37 °C and 5% CO_2 in a humidified atmosphere. For subcultivation, cells at 75% -90% confluency were detached from the cell culture dish (*via* scraping or accutase treatment for macrophages, *via* trypsin treatment for HEK and CHO cells), and an appropriate aliquot was transferred to a new dish and medium. For macrophages, 5×10^4 cells/well were seeded in 96-well plates, and 7.5×10^5 cells/well in 6-well plates for experiments that were started 16–24 h later. For induction of M1 polarization, macrophages were stimulated with 100 ng/mL lipopolysaccharide (stock: 1 mg/mL in water; Sigma Aldrich, Austria). Treatment with test compounds usually preceded the LPS stimulus by 15 min unless stated otherwise. All compounds were applied as a stock solution in DMSO. Solvent concentration was even throughout all samples of one experiment and never exceeded 0.3%.

2.3 Determination of extracellular NO and cell viability

Cells were seeded in 96-well plates and treated with geraniin, urolithin A and LPS as indicated (final volume/well: 200 μL). After 24 h 100 μL of the supernatants were removed and mixed 1:1 with freshly prepared Griess reagent (0.05% naphthylendiamine, 0.5% sulfanilamide, 2.5% H_3PO_4 in water) to determine nitrite as surrogate readout for NO release. Absorbance of the pink azo-dye was assessed at 550 nm. To the cells (still covered with 100 μL medium), 100 μL of the ready-to-go Cell TiterGlo solution (Promega, Austria) were added, the plate was incubated in the dark for 1 h and then luminescence was recorded using a multiplate reader (Tecan, Austria).

2.4 Determination of intracellular reactive oxygen species (ROS)

Cells were treated as desired and then exposed to the ROS sensitive dye H_2DCF-DA (20 μM) for 30 min. Cells were washed and mean green fluorescence of 20,000 cells /sample was analyzed by flow cytometry (FL1 channel) with a FACSCalibur™ (BD Biosciences, Austria) instrument. Obtained values were corrected for autofluorescene of control cells without dye.

2.5 Western blot analysis

After the desired cell treatment extraction of total cell lysates, SDS-polyacrylamide electrophoresis and immunoblot analysis were performed essentially as described previously [32]. To separate nuclear from cytosolic proteins, cells were first washed with cold PBS and then exposed to buffer 1 (10 mM HEPES pH 7.5, 0.2 mM EDTA, 10 mM KCl, 1% NP40 (Igepal), 1 mM DTT, 0.5 mM PMSF, CompleteTM (Roche, Switzerland)). Cells were scraped off and transferred into a microtube and incubated for 15 min on ice, with vigorous vortexing every 2–3 min, and centrifuged for 5 min at 11000*g*. The supernatant was collected as cytosolic fraction. The obtained pellets were washed once with buffer 1 and were then resuspended in buffer 2 (20 mM HEPES pH 7.5, 1.1 mM EDTA, 420 mM NaCl, 1 mM DTT, PMSF and Complete™ (Roche, Switzerland)) incubated on ice for 15 min with vigorous vortexing every 2–3 min, followed by centrifugation for 5 min at 11000*g*. The supernatant contained nuclear proteins. Successful separation of cytosolic and nuclear fractions was routinely validated by immunoblotting of tubulin (cytosolic marker) and lamin (nuclear marker), respectively.

2.6 Reporter gene assays

Peroxisome proliferator activated receptor (PPAR)γ, liver X receptors (LXR) α,β and retinoid X receptor (RXR)α reporter gene assays utilized HEK293 cells that were transiently transfected with the expression plasmid and response element of the respective nuclear receptor as well as a plasmid coding for enhanced green fluorescent protein (EGFP) as control. The nuclear factor erythroid 2 related factor 2 (Nrf2)-dependent reporter gene assay was done in CHO cells stably expressing an ARE-dependent luciferase reporter gene and a control EGFP expression plasmid. The procedure was essentially the one described in previous studies [31,33,34].

2.7 Confocal laser scanning microscopy

Cells were grown on coverslips and treated as indicated. The coverslips were then washed with PBS and cells were fixed with 3.7% formaldehyde in PBS followed by permeabilization with 0.5% Triton® X-100 in PBS. After two washing steps with PBS, the coverslips were incubated with blocking solution (2% BSA in PBS) for 30 min, then with anti-p65 antibody (1:50 in PBS/BSA) for two hours, washed and then exposed to FITC-coupled anti-rabbit antibody (1:500 in PBS/BSA) for another hour. After washing, the coverslips were mounted on a glass slide using ProLong antifade-mounting medium (New England Biolabs, Germany) and kept at 4 °C overnight. Confocal laser scanning microscopy was performed using a TCS SP5 II system (Leica, Germany). Images were recorded with a 63× oil immersion objective using the manufacturer's LAS AF imaging software. All

compared samples within one experiment were detected with constant gain, zoom and exposure time.

2.8 Statistics

Experiments were performed at least three times. Error bars in the pictures represent the standard deviation (SD). Statistical significance was determined by using Student's *t*-test (for two groups) or ANOVA (> 2 groups) followed by Dunnett's or Bonferroni's post test in the GraphPad Prism software. p-values < 0.05 were considered as significant and are designated with * in the figures.

3 Results

3.1 Urolithin A is more potent in impeding M1(LPS) macrophage polarization than geraniin

In a first step, we compared the influence of geraniin and urolithin A (Fig. 1a) side by side on M1 macrophage polarization. As expected, the employed murine J774.1 macrophages responded to stimulation with 100 ng/mL LPS with an augmented production of NO. The NO release could be suppressed by geraniin and urolithin A in a concentration-dependent manner, as shown by the results from a Griess assay in Fig. 1b. In more detailed concentration-response experiments urolithin showed an apparent IC_{50} value of 14 μM whereas geraniin reached 50% inhibition only at around 40 μM. The values are comparable to those from studies focusing on the individual compounds and using RAW264.7 macrophages [21,35]. Cell viability was not markedly affected by urolithin A and geraniin in LPS-stimulated macrophages compared to control cells, as assessed by an ATP–based luminescent viability assays (Fig. 1c), and complementary MTT (3-(4,5-Dimethylthiazol-2-yl)-2,5-diphenyltetrazoliumbromid)-, resazurin-(both metabolic activity) and crystal violet (biomass) assays (data not shown). Next to NO, LPS-stimulated macrophages produced more ROS compared to naïve macrophages. Again, the test compounds were able to counter the ROS production, and urolithin A was more potent than geraniin (Fig. 1d). LPS further triggered induction of iNOS, Cox-2 and pro-IL1β expression in macrophages which were diminished by 40 μM urolithin A, with a stronger effect on pro-IL-1β and iNOS than on Cox2 (Fig. 1e–g). Geraniin at 40 μM reduced LPS-induced iNOS-, but not IL-1β and Cox2 expression. Inflammasome activation as assessed by levels of mature IL-1β and cleaved caspase1 was not obviously altered in LPS-primed (4 h) macrophages upon nigericin-trigger (45 min) in the presence of either compound (data not shown). Overall, LPS stimulation led to a pro-inflammatory M1 polarization in J774.1 macrophages (from now on also referred to M1(LPS)) which is characterized by elevated pro-IL-1β, iNOS- and Cox2 expression, massive NO release and increased ROS production. A direct side by side comparison revealed that the metabolite urolithin A hinders the M1(LPS) polarization and is hereby more potent and versatile than the parent ellagitannin geraniin, suggesting that microbial metabolization boosts the anti-inflammatory potential.

3.2 Urolithin A and geraniin have no influence on peroxisome proliferator activated receptor (PPAR)γ, liver X receptors (LXR), retinoid X receptor α (RXR) or nuclear factor erythroid 2 related factor 2 (Nrf2)-mediated gene transactivation

The anti-inflammatory properties of Urolithin A and geraniin have been mainly assigned to an impaired nuclear factor κ B (NF-κB) signaling in previous studies [21,36]. However, other anti-inflammatory targets have not been investigated to a great extent. We therefore examined potential agonism of geraniin and urolithin A on nuclear receptors with anti-inflammatory properties. Those studies included PPARγ, LXR α and β, which counter pro-inflammatory gene expression and seem to determine macrophage polarization also by controlling lipid metabolism [37–39] as well as RXRα, the heterodimerization partner of the permissive PPAR and LXR. However, neither geraniin nor urolithin A was able to markedly activate luciferase expression in the respective reporter gene assay, whereas the used positive controls (pioglitazone for PPARγ, GW 3965 for the LXRs and retinoic acid for RXR) elicited significant activation. (Fig. 2a–d). At 50 μM, urolithin A was able to slightly (approx. 2-fold induction) elevate the RXRα-dependent luciferase signal (Fig. 2d). However, compared to the positive control retinoic acid (approx. 35-fold induction) the effect was considered to be hardly relevant. Nrf2 is a stress responsive and antioxidant transcription factor also showing anti-inflammatory activity [40,41]. Using a Nrf2-dependent luciferase reporter gene assay (antioxidant-response element (ARE)-LUC) we did not observe increased Nrf2 signaling with urolithin A or geraniin, while the positive control CDDO-IM elicited a strong luciferase signal (Fig. 2e). Overall, geraniin and urolithin A did not show marked activation of PPAR, LXR, RXR or Nrf2. Based on the finding that urolithin A was more efficient in prevention of M1(LPS) macrophage polarization (and presumably more relevant when thinking of the *in vivo* situation) than geraniin, we focused on a better characterization and understanding of the anti-inflammatory activity of urolithin A.

3.3 Urolithin A leads to an elevated autophagic flux in macrophages

A recent study reported life span prolongation in the nematode *C. elegans* by urolithin A-mediated induction of autophagy [42]. The authors also investigated induction of autophagy in myo- and hepatocytes, but not in macrophages. To close this gap and because autophagy and immunomodulation are linked phenomena [43–45], we examined the autophagic flux in macrophages upon exposure to urolithin A *in vitro*. The level of lipidated microtubule-associated protein 1A/1B-light chain 3 (LC3; the lipidated form LC3II) was determined in macrophages by western blot analysis after treatment with urolithin A (40 μM) and rapamycin (250 nM, positive control) in the presence and absence of bafilomycin, an inhibitor of vacuolar ATPase and autophagosome fusion with the lysosome. In the presence of bafilomycin urolithin A significantly increased the LC3II level compared to DMSO, indicating an increased autophagic flux in naïve and LPS-stimulated macrophages (Fig. 3a) [46]. As expected, the mTOR inhibitor rapamycin also led to an increased autophagic flux. Moreover, the pro-autophagic effect of urolithin A occurred in a concentration dependent manner (Fig. 3b). Thus, urolithin A is able to enhance the autophagic flux in macrophages.

3.4 Urolithin A interferes with the Akt/mTOR signaling pathway

Autophagy is a highly regulated and finely tuned complex process that integrates cues from a plethora of signaling molecules. However, mTOR and AMP-activated kinase (AMPK) are considered as main control hubs of autophagy [47–50]. Time course experiments revealed that LPS-treatment leads to an increase in the Akt/mTOR/p70 S6K signaling axis after approximately 1 h in macrophages that lasts up to 8 h (Suppl Fig. 1). An increased phosphorylation and activation of AKT is transduced to an increased phosphorylation of tuberin (TSC2) at threonine 1462 which in turn leads to activation of the mTOR complex *via* the small G-protein Rheb. Activated mTOR finally phosphorylates its substrates including p70S6K at Ser 389 [51]. In order to examine the influence of urolithin A on the mTOR signaling pathway, macrophages were treated with 20 and 40 μM urolithin A in the absence or presence of LPS for 2 and 6 h. Subsequent western blot analysis of total cell lysates revealed that urolithin A was able to suppress LPS-induced AKT, TSC2 and as well as basal and LPS-induced p70S6K phosphorylation (Fig. 4a–c). In contrast, levels of phosphorylated (Ser79) acetyl-CoA carboxylase (ACC) as readout for AMPK activity did not obviously change between control and urolithin A -treated cells (Suppl. Fig. 2). Thus, urolithin A is able to interfere with the mTOR signaling pathway in macrophages which is likely to account for the observed increase in autophagic flux.

3.5 The increased autophagic flux contributes to the prevention of M1(LPS) macrophage polarization by urolithin A

In a next step we examined whether the increased autophagic flux is linked with the anti-inflammatory activity of urolithin A. The most primordial function of autophagy is adaptation to nutrient deprivation. However, the autophagy machinery has also been found to entangle with immunity and inflammation [43–45]. Monitoring LPS-triggered NO production uncovered inhibition by urolithin A (in line with Fig. 1) at 10 to 50 μM which was completely abrogated in the presence of the autophagy inhibitor bafilomycin at 10 and 100 nM (Fig. 5a). A similar picture became apparent for LPS-induced iNOS, Cox2 and pro-IL-1β expression, which were blunted in a concentration-dependent manner by urolithin A (suppression of pro-IL-1β only significant at 40 μM). Addition of bafilomycin diminished the inhibitory capacity of 40 μM urolithin A by at least 50% (Fig. 5b). Notably, bafilomycin on its own negatively affected the extent of pro-IL1β-induction by LPS. Taken together, these findings indicate that the increased autophagic flux contributes to the alleviated M1 (LPS) macrophage polarization by urolithin A.

3.6 The increased autophagic flux appears pivotal for the impeded nuclear translocation in the presence of urolithin A

NF-κB signaling, one main mediator of the M1(LPS) polarization in murine macrophages, is negatively affected by urolithin A. Previous reports showed that urolithin A reduced nuclear translocation and DNA binding of NF-κB [21]. Degradation of inhibitor of NF-κB (IκB), which usually precedes nuclear translocation of NF-κB and becomes most apparent after 30 min of LPS stimulation, is not influenced (Fig. 6a), suggesting that urolithin A acts between release from its inhibitor IκB and nuclear translocation of the p65 Rel protein (one transactivating member of the NF-κB protein family). Thus, we went on to investigate the

relationship between increased autophagy and inhibited nuclear accumulation of p65 (NF-κB) in urolithin A-treated macrophages. One hour after LPS stimulation appeared as optimal time point to study nuclear p65 in the used murine macrophages (Suppl. Fig. 3). Employing confocal laser scanning microscopy (Fig. 6b) and western blot analysis of nuclear extracts (Fig. 6c) confirmed that urolithin A impedes nuclear accumulation of p65. Of note, co-treatment with the autophagy inhibitor bafilomycin overcame the blunted nuclear translocation of p65 by urolithin A. Bafilomycin alone had no influence on nuclear p65 levels. These data imply that urolithin A interferes with NF-κB (p65) function at a step between release from the IκB complex and transport into the nucleus in an autophagy-dependent manner.

4 Discussion

The main findings of this study are that (i) microbial metabolization of geraniin to urolithin A increases the anti-inflammatory potential, (ii) urolithin A triggers an increased autophagic flux in macrophages which contributes to reduced nuclear abundance of p65 (NF-κB) and M1(LPS) polarization and that (iii) urolithin A exerts a negative influence on the AKT/TSC/mTOR signaling axis.

The concept that the intestinal microbiome is a critical player in metabolization and exploitation of ingested food and drugs is commonly accepted. For instance, metabolization of dietary fiber (precursor) into short chain fatty acids (active principle), such as butyric acid acting mainly as epigenetic modulator, is thought to bring about the benefits of a fiber-rich diet [52,53]. Secondary plant metabolites often show promising bioactivity *in vitro* but very low bioavailability *in vivo*. Nonetheless, ellagitannin supplementation or diets rich in pomegranate, berries or nuts have been positively correlated with health benefits (*e.g.* [54,55]). The active principles beyond these effects are likely metabolites. Orally consumed ellagitannins are hydrolyzed in the gut to release ellagic acid, which in turn is further processed by certain gut bacteria into a series of urolithins with distinct hydroxylation pattern, that then are subject of phase 2 metabolism by enterocytes and hepatocytes. This yields glucuronides, sulfates and methyl derivatives of urolithins which appear in the circulation at nM to low μM concentrations. Prevalent metabolites in humans are conjugates with glucuronic acid of urolithin A, isourolithin A and urolithin B. These circulate in human plasma with huge interindividual variability in the range of 0.024–35 μM for urolithin A-glucuronide, 0.0045–0.745 μM for isourolithin-A glucuronide and 0.012–73 μM for urolithin B-glucuronide, depending on study design. Under a dietary approach it is unlikely that substantial amounts of free urolithin aglycones reach the systemic circulation. Local tissue distribution ranged from 2 ng/g urolithin A glucuronide in prostate and 4.8 to 507,3 ng/g for several aglycones and conjugates in colon (reviewed in [56,57]). A recent study in rats measured plasma levels of urolithin A upon intraperitoneal administration of 2.5 mg/kg/day and only found up to 0.015 μM urolithin A and 0.39 μM urolithin A-sulfate in plasma, up to 10 nmol aglycone and up to 60 nmol sulfate per gram tissue in heart, pancreas and liver [58]. Based on these findings one is generally advised to use a mixture of appropriate urolithin conjugates for *in vitro* studies on endothelial cells and systemic tissues, whereas aglycones could be more suitable for cell types resident in colon. Urolithin concentrations in the two-digit μmolar range as used in this study might be justified for

individual aglycones or conjugates, but need to be carefully chosen according to available data, cell type of interest as well as the difference between the dietary scenario and a pharmacological setting in which high doses of synthetic urolithins are given intraperitoneally or intravenously. In this line, our future studies can benefit from investigating (a mixture of) urolithin metabolites (glucuronides and sulfates) in order to have relevant *in vitro* data with regard to systemic inflammation, as well as from working with a mixture of urolithin aglycones for statements with potential relevance for colon-resident macrophages. Working with mixtures would also take into account the important point of potential synergistic effects between the individual compounds. A recent study by Piwowarksi et al. [59] suggested the intriguing novel concept that the phase 2 conjugates of urolithin serve as prodrug that could be deconjugated to the aglycones at sites of inflammation and malignant transformation due to low pH and/or elevated glucuronidase activity. Thus, it seems that the jury is still out to decide which metabolite at what concentration ultimately qualifies for the active principle of the systemic positive effects of ellagitannins in inflammation and cancer.

In contrast to punicalagin (another ellagitannin) [60] neither urolithin A nor geraniin promoted the M2 polarization in the employed murine macrophages as arginase 1 expression was not increased (data not shown). However, geraniin but not urolithin A boosted LPS-induced expression of heme-oxygenase-1, a potential anti-inflammatory protein involved in the M2 polarization and resolution of inflammation [60] (Suppl. Fig. 4). This suggests that the metabolization of geraniin may abolish the capability of triggering a potential M1 → M2 shift counter-balancing the inflammatory response upon LPS stimulation (which, however, may become obsolete due to the already strong impediment of an initial M1(LPS) polarization by urolithin A in the first place).

Autophagy and immunomodulation are interdependent in the cellular network of signal integration (*e.g.* [61–63]). Our study shows that an increased autophagic flux contributes to the anti-inflammatory action of urolithin A. Urolithin A impedes M1 (LPS) macrophage polarization (inhibition of iNOS/Cox2/pro-IL-1β expression, NO and ROS release) and triggers an elevated autophagic flux. Inhibition of the autophagic flux by bafilomycin blunted the anti-inflammatory activity of urolithin A, indicating an actual cross-talk between both processes. Knockdown of vital players in the autophagic machinery (such as autophagy gene (Atg) 5 or beclin) should complement the pharmacological approach and unambiguously corroborate the autophagy/anti-inflammation link in the activity profile of urolithin A, optimally in primary macrophages. Inhibition of the M1(LPS) polarization in macrophages by urolithin A could previously be traced back to inhibition of the NF-κB signaling pathway [21]. Our study defined the point of action of urolithin A as located between release from IκB and nuclear translocation of p65 and as susceptible to autophagic signaling. Impeded autophagy restored nuclear translocation of p65 also in the presence of urolithin A. Future experiments will address the obvious question how an increased pro-autophagic signaling can interfere with nuclear translocation of p65 in M1(LPS) macrophages.

Geraniin and urolithin A did not show a marked agonism on the nuclear receptors PPARγ, RXRα and LXRα/β or on activation of the stress responsive transcription factor Nrf2. Their

polar nature may prevent binding to the nuclear receptors that usually habour lipopilic ligands, such fatty acids or sterols. Accordingly, in endothelial cells urolithin A led to increased PPARγ expression rather than acted as ligand [64]. The putative positive impact on PPARγ signaling due to increased abundance could not be confirmed in macrophages, though, as we did not see increased PPARγ levels nor target gene expression upon urolithin A exposure (data not shown). Although reported for geraniin in previous studies [35,65], we did not observe any activation of Nrf2 signaling with urolithin A or geraniin. The reasons for the divergent results on geraniin may be based on the different readouts for Nrf2 activation (Nrf2 accumulation/heme oxygenase 1 expression) [35] *versus* consensus sequence-based reporter gene assays (ARE-LUC (here)), different experimental setups (pre-stressed cells [35] *versus* naïve cells (here)) or an actual metabolite of geraniin being the active principle for Nrf2 activation in the *in vivo* setting [65].

Looking at the two major prominent control hubs in autophagy, we showed unaltered AMPK activity but impaired mTOR signaling in urolithin-treated cells. Phosphorylation of p70 S6K, indicative for an active mTOR signaling, was strongly and concentration-dependently decreased by urolithin A treatment in naïve and LPS-stimulated macrophages. Therefore, induction of autophagy is likely to occur *via* an inhibited mTOR axis in urolithin-exposed M1(LPS) macrophages. Notably, mTOR inhibition occurred as anti-inflammatory strategy in several recent publications (*e.g.* [66,67]), but was also found to aggravate (adipose tissue) inflammation in other studies [68,69]. More studies are needed to completely decipher the context-and tissue specific action of mTOR in inflammation, to understand the possible distinct responses to pharmacological mTOR inhibition and absolute mTOR deficiency as well as the detailed mode of action underlying the augmented autophagic flux upon urolithin A. Urolithin A also increased the life span of the nematode *C. elegans via* increased autophagy [42], and was reported to inhibit proliferation of various cancer cell lines, to exert vaso- and cardioprotective effects or improve lipid profiles [18,19,58,64,70,71]. To what extent autophagy induction plays a role for these effects has not been investigated so far although there is good chance that autophagy is involved [72–74].

Given the wide-spread and long-term dietary exposure to their metabolic precursors, urolithins have been comparatively poorly characterized concerning their biological effects. A recent study has assessed safety and determined the NOAEL (no observed adverse effect level) for the daily oral intake of urolithin A as 3.4 (female) to 3.8 (male) g/per kg body weight [75]. Only for a decade research efforts have been providing a better understanding of the molecular mechanism of these metabolites. We could complement the arising picture by showing that urolithin A possesses a higher anti-inflammatory potential *in vitro* than the precursor ellagitannin geraniin and increases the autophagic flux which in turn blocks nuclear translocation of p65 and M1(LPS) polarization in macrophages. Future *in vitro* and *in vivo* studies are warranted to fully capture and appreciate the potential health benefit obtained from ellagitannins and their metabolites as well as the synergy between nutrition, host cells and gut microbiota (*e.g.* [76]).

Appendix A. Supplementary data

Refer to Web version on PubMed Central for supplementary material.

Acknowledgments

The authors thank Drs. Simone Latkolik and Angela Ladurner, University of Vienna, for her initial help with reporter gene assays in HEK cells. This work was supported by the FWF (P29392 to EHH), the Herzfelder Jubiläumsstiftung (to EHH) and a Willmar Schwabe research fellowship from the Society of Medicinal Plant and Natural Product Research (to YDB).

References

[1]. Agyare C, et al. An ethnopharmacological survey and in vitro confirmation of ethnopharmacological use of medicinal plants used for wound healing in Bosomtwi-Atwima-Kwanwoma area, Ghana. J Ethnopharmacol. 2009; 125:393–403. DOI: 10.1016/j.jep.2009.07.024 [PubMed: 19635544]

[2]. Boakye YD, Agyare C, Abotsi WK, Ayande PG, Ossei PP. Anti-inflammatory activity of aqueous leaf extract of *Phyllanthus muellerianus* (Kuntze) Exell. and its major constituent, geraniin. J Ethnopharmacol. 2016; 187:17–27. DOI: 10.1016/j.jep.2016.04.020 [PubMed: 27103113]

[3]. Cheng HS, Ton SH, Kadir KA. Ellagitannin geraniin: a review of the natural sources, biosynthesis, pharmacokinetics and biological effects. Phytochem Rev. 2017; 16:159–193. DOI: 10.1007/s11101-016-9464-2

[4]. Ito H. Metabolites of the ellagitannin geraniin and their antioxidant activities. Planta Med. 2011; 77:1110–1115. DOI: 10.1055/s-0030-1270749 [PubMed: 21294073]

[5]. Ito H, Iguchi A, Hatano T. Identification of urinary and intestinal bacterial metabolites of ellagitannin geraniin in rats. J Agric Food Chem. 2008; 56:393–400. DOI: 10.1021/jf0726942 [PubMed: 18163562]

[6]. Agyare C, Lechtenberg M, Deters A, Petereit F, Hensel A. Ellagitannins from *Phyllanthus muellerianus* (Kuntze) Exell.: geraniin and furosin stimulate cellular activity, differentiation and collagen synthesis of human skin keratinocytes and dermal fibroblasts. Phytomedicine. 2011; 18:617–624. DOI: 10.1016/j.phymed.2010.08.020 [PubMed: 21036574]

[7]. Yang CM, Cheng HY, Lin TC, Chiang LC, Lin CC. The in vitro activity of geraniin and 1,3,4,6-tetra-O-galloyl-beta-d-glucose isolated from *Phyllanthus urinaria* against herpes simplex virus type 1 and type 2 infection. J Ethnopharmacol. 2007; 110:555–558. DOI: 10.1016/j.jep.2006.09.039 [PubMed: 17113739]

[8]. Yang Y, Zhang L, Fan X, Qin C, Liu J. Antiviral effect of geraniin on human enterovirus 71 in vitro and in vivo. Bioorg Med Chem Lett. 2012; 22:2209–2211. DOI: 10.1016/j.bmcl.2012.01.102 [PubMed: 22342145]

[9]. Liu C, et al. Identification of hydrolyzable tannins (punicalagin, punicalin and geraniin) as novel inhibitors of hepatitis B virus covalently closed circular DNA. Antivir Res. 2016; 134:97–107. DOI: 10.1016/j.antiviral.2016.08.026 [PubMed: 27591143]

[10]. Zhai JW, et al. Geraniin induces apoptosis of human breast cancer cells MCF-7 via ROS-mediated stimulation of p38 MAPK. Toxicol Mech Methods. 2016; 26:311–318. DOI: 10.3109/15376516.2016.1139025 [PubMed: 27097871]

[11]. Wang X, et al. Geraniin suppresses ovarian cancer growth through inhibition of NF-kappaB activation and downregulation of Mcl-1 expression. J Biochem Mol Toxicol. 2017; doi: 10.1002/jbt.21929

[12]. Aayadi H, Mittal SPK, Deshpande A, Gore M, Ghaskadbi SS. Protective effect of geraniin against carbon tetrachloride induced acute hepatotoxicity in Swiss albino mice. Biochem Biophys Res Commun. 2017; 487:62–67. DOI: 10.1016/j.bbrc.2017.04.013 [PubMed: 28396147]

[13]. Londhe JS, Devasagayam TP, Foo LY, Shastry P, Ghaskadbi SS. Geraniin and amariin, ellagitannins from *Phyllanthus amarus*, protect liver cells against ethanol induced cytotoxicity. Fitoterapia. 2012; 83:1562–1568. DOI: 10.1016/j.fitote.2012.09.003 [PubMed: 22982332]

[14]. Youn K, Jun M. In vitro BACE1 inhibitory activity of geraniin and corilagin from *Geranium thunbergii*. Planta Med. 2013; 79:1038–1042. DOI: 10.1055/s-0032-1328769 [PubMed: 23877922]

[15]. Wang P, et al. Geraniin exerts cytoprotective effect against cellular oxidative stress by upregulation of Nrf2-mediated antioxidant enzyme expression via PI3K/AKT and ERK1/2

pathway. Biochim Biophys Acta. 2015; 1850:1751–1761. DOI: 10.1016/j.bbagen.2015.04.010 [PubMed: 25917210]

[16]. Bing SJ, et al. Geraniin down regulates gamma radiation-induced apoptosis by suppressing DNA damage. Food Chem Toxicol. 2013; 57:147–153. DOI: 10.1016/j.fct.2013.03.022 [PubMed: 23541438]

[17]. Okabe S, et al. New TNF-alpha releasing inhibitors, geraniin and corilagin, in leaves of Acer nikoense, Megusurino-ki. Biol Pharm Bull. 2001; 24:1145–1148. [PubMed: 11642320]

[18]. Zhou B, Wang J, Zheng G, Qiu Z. Methylated urolithin A, the modified ellagitannin-derived metabolite, suppresses cell viability of DU145 human prostate cancer cells via targeting miR-21. Food Chem Toxicol. 2016; 97:375–384. DOI: 10.1016/j.fct.2016.10.005 [PubMed: 27725205]

[19]. Zhang W, et al. Urolithin A suppresses the proliferation of endometrial cancer cells by mediating estrogen receptor-alpha-dependent gene expression. Mol Nutr Food Res. 2016; 60:2387–2395. DOI: 10.1002/mnfr.201600048 [PubMed: 27342949]

[20]. Teixeira LL, et al. Potential antiproliferative activity of polyphenol metabolites against human breast cancer cells and their urine excretion pattern in healthy subjects following acute intake of a polyphenol-rich juice of grumixama (*Eugenia brasiliensis* Lam.). Food Funct. 2017; 8:2266–2274. DOI: 10.1039/c7fo00076f [PubMed: 28541359]

[21]. Piwowarski JP, Kiss AK, Granica S, Moeslinger T. Urolithins, gut microbiota-derived metabolites of ellagitannins, inhibit LPS-induced inflammation in RAW 264.7 murine macrophages. Mol Nutr Food Res. 2015; 59:2168–2177. DOI: 10.1002/mnfr.201500264 [PubMed: 26202092]

[22]. Piwowarski JP, et al. Role of human gut microbiota metabolism in the anti-inflammatory effect of traditionally used ellagitannin-rich plant materials. J Ethnopharmacol. 2014; 155:801–809. DOI: 10.1016/j.jep.2014.06.032 [PubMed: 24969824]

[23]. Motwani MP, Gilroy DW. Macrophage development and polarization in chronic inflammation. Semin Immunol. 2015; 27:257–266. DOI: 10.1016/j.smim.2015.07.002 [PubMed: 26216597]

[24]. Baseler WA, et al. Autocrine IL-10 functions as a rheostat for M1 macrophage glycolytic commitment by tuning nitric oxide production. Redox Biol. 2016; 10:12–23. DOI: 10.1016/j.redox.2016.09.005 [PubMed: 27676159]

[25]. Soehnlein O, Lindbom L. Phagocyte partnership during the onset and resolution of inflammation. Nat Rev Immunol. 2010; 10:427–439. DOI: 10.1038/nri2779 [PubMed: 20498669]

[26]. Davies LC, Taylor PR. Tissue-resident macrophages: then and now. Immunology. 2015; 144:541–548. DOI: 10.1111/imm.12451 [PubMed: 25684236]

[27]. Esser N, Legrand-Poels S, Piette J, Scheen AJ, Paquot N. inflammation as a link between obesity, metabolic syndrome and type 2 diabetes. Diabetes Res Clin Pract. 2014; 105:141–150. DOI: 10.1016/j.diabres.2014.04.006 [PubMed: 24798950]

[28]. VanItallie TB. Alzheimer's disease: innate immunity gone awry? Metabolism. 2017; 69S:S41–S49. DOI: 10.1016/j.metabol.2017.01.014 [PubMed: 28129888]

[29]. Kim H, et al. Pomegranate polyphenolics reduce inflammation and ulceration in intestinal colitis-involvement of the miR-145/p70S6K1/HIF1alpha axis in vivo and in vitro. J Nutr Biochem. 2017; 43:107–115. DOI: 10.1016/j.jnutbio.2017.02.005 [PubMed: 28282584]

[30]. Kim H, et al. Comparison of anti-inflammatory mechanisms of mango (*Mangifera indica* L.) and pomegranate (*Punica granatum* L.) in a preclinical model of colitis. Mol Nutr Food Res. 2016; 60:1912–1923. DOI: 10.1002/mnfr.201501008 [PubMed: 27028006]

[31]. Kropat C, et al. Modulation of Nrf2-dependent gene transcription by bilberry anthocyanins in vivo. Mol Nutr Food Res. 2013; 57:545–550. DOI: 10.1002/mnfr.201200504 [PubMed: 23349102]

[32]. Zimmermann K, et al. Activated AMPK boosts the Nrf2/HO-1 signaling axis—a role for the unfolded protein response. Free Radic Biol Med. 2015; 88:417–426. DOI: 10.1016/j.freeradbiomed.2015.03.030 [PubMed: 25843659]

[33]. Atanasov AG, et al. Honokiol: a non-adipogenic PPARgamma agonist from nature. Biochim Biophys Acta. 2013; 1830:4813–4819. DOI: 10.1016/j.bbagen.2013.06.021 [PubMed: 23811337]

[34]. Temml V, Voss CV, Dirsch VM, Schuster D. Discovery of new liver X receptor agonists by pharmacophore modeling and shape-based virtual screening. J Chem Inf Model. 2014; 54:367–371. DOI: 10.1021/ci400682b [PubMed: 24502802]

[35]. Wang P, et al. Inhibitory effects of geraniin on LPS-induced inflammation via regulating NF-kappaB and Nrf2 pathways in RAW 264.7 cells. Chem Biol Interact. 2016; 253:134–142. DOI: 10.1016/j.cbi.2016.05.014 [PubMed: 27181634]

[36]. Guada M, Ganugula R, Vadhanam M, Majeti RK. Urolithin A mitigates cisplatin-induced nephrotoxicity by inhibiting renal inflammation and apoptosis in an experimental rat model. J Pharmacol Exp Ther. 2017; doi: 10.1124/jpet.117.242420

[37]. Delerive P, Fruchart JC, Staels B. Peroxisome proliferator-activated receptors in inflammation control. J Endocrinol. 2001; 169:453–459. [PubMed: 11375115]

[38]. Chinetti G, Fruchart JC, Staels B. Peroxisome proliferator-activated receptors (PPARs): nuclear receptors at the crossroads between lipid metabolism and inflammation. Inflamm Res. 2000; 49:497–505. DOI: 10.1007/s000110050622 [PubMed: 11089900]

[39]. Schulman IG. Liver X receptors link lipid metabolism and inflammation. FEBS Lett. 2017; doi: 10.1002/1873-3468.12702

[40]. Li N, Nel AE. Role of the Nrf2-mediated signaling pathway as a negative regulator of inflammation: implications for the impact of particulate pollutants on asthma. Antioxid Redox Signal. 2006; 8:88–98. DOI: 10.1089/ars.2006.8.88 [PubMed: 16487041]

[41]. Reuter S, Gupta SC, Chaturvedi MM, Aggarwal BB. Oxidative stress, inflammation, and cancer: how are they linked? Free Radic Biol Med. 2010; 49:1603–1616. DOI: 10.1016/j.freeradbiomed.2010.09.006 [PubMed: 20840865]

[42]. Ryu D, et al. Urolithin A induces mitophagy and prolongs lifespan in *C. elegans* and increases muscle function in rodents. Nat Med. 2016; 22:879–888. DOI: 10.1038/nm.4132 [PubMed: 27400265]

[43]. Heymann D. Autophagy: a protective mechanism in response to stress and inflammation. Curr Opin Investig Drugs. 2006; 7:443–450.

[44]. Levine B, Deretic V. Unveiling the roles of autophagy in innate and adaptive immunity. Nat Rev Immunol. 2007; 7:767–777. DOI: 10.1038/nri2161 [PubMed: 17767194]

[45]. Deretic V. Links between autophagy, innate immunity, inflammation and Crohn's disease. Dig Dis. 2009; 27:246–251. DOI: 10.1159/000228557 [PubMed: 19786748]

[46]. Klionsky DJ, et al. Guidelines for the use and interpretation of assays for monitoring autophagy (3rd edition). Autophagy. 2016; 12:1–222. DOI: 10.1080/15548627.2015.1100356 [PubMed: 26799652]

[47]. Diaz-Troya S, Perez-Perez ME, Florencio FJ, Crespo JL. The role of TOR in autophagy regulation from yeast to plants and mammals. Autophagy. 2008; 4:851–865. [PubMed: 18670193]

[48]. Jung CH, Ro SH, Cao J, Otto NM, Kim DH. mTOR regulation of autophagy. FEBS Lett. 2010; 584:1287–1295. DOI: 10.1016/j.febslet.2010.01.017 [PubMed: 20083114]

[49]. Carroll B, Dunlop EA. The lysosome: a crucial hub for AMPK and mTORC1 signalling. Biochem J. 2017; 474:1453–1466. DOI: 10.1042/BCJ20160780 [PubMed: 28408430]

[50]. Yao F, Zhang M, Chen L. 5′-Monophosphate-activated protein kinase (AMPK) improves autophagic activity in diabetes and diabetic complications. Acta Pharm Sin B. 2016; 6:20–25. DOI: 10.1016/j.apsb.2015.07.009 [PubMed: 26904395]

[51]. Laplante M, Sabatini DM. mTOR signaling in growth control and disease. Cell. 2012; 149:274–293. DOI: 10.1016/j.cell.2012.03.017 [PubMed: 22500797]

[52]. Davie JR. Inhibition of histone deacetylase activity by butyrate. J Nutr. 2003; 133:2485S–2493S. [PubMed: 12840228]

[53]. O'Keefe SJ. Diet, microorganisms and their metabolites, and colon cancer. Nat Rev Gastroenterol Hepatol. 2016; 13:691–706. DOI: 10.1038/nrgastro.2016.165 [PubMed: 27848961]

[54]. Sangiovanni E, et al. Ellagitannins from Rubus berries for the control of gastric inflammation: in vitro and in vivo studies. PLoS One. 2013; 8:e71762.doi: 10.1371/journal.pone.0071762 [PubMed: 23940786]

[55]. Jean-Gilles D, et al. Anti-inflammatory effects of polyphenolic-enriched red raspberry extract in an antigen-induced arthritis rat model. J Agric Food Chem. 2012; 60:5755–5762. DOI: 10.1021/jf203456w [PubMed: 22111586]

[56]. Tomas-Barberan FA, et al. Urolithins, the rescue of “old”metabolites to understand a “new” concept: metabotypes as a nexus among phenolic metabolism, microbiota dysbiosis, and host health status. Mol Nutr Food Res. 2017; 61 xx. doi: 10.1002/mnfr.201500901

[57]. Espin JC, Larrose M, Garcia-Conesa MT, Tomas-Barberan F. Biological significance of urolithins, the gut microbial ellagic-acid-derived metabolites: the evidence so far. Evid Based Complement Alternat Med. 2013; 2013:270418.doi: 10.1155/2013/270418 [PubMed: 23781257]

[58]. Savi M, et al. In vivo administration of urolithin A and B prevents the occurrence of cardiac dysfunction in streptozotocin-induced diabetic rats. Cardiovasc Diabetol. 2017; 16:80.doi: 10.1186/s12933-017-0561-3 [PubMed: 28683791]

[59]. Piwowarski JP, Stanisławska I, Granica S, Stefańska J, Kiss AK. Phase II conjugates of urolithins isolated from human urine and potential role of β-glucuronidases in their disposition. Drug Metab Dispos. 2017; 45:657–665. DOI: 10.1124/dmd.117.075200 [PubMed: 28283501]

[60]. Xu X, et al. Punicalagin, a PTP1B inhibitor, induces M2c phenotype polarization via up-regulation of HO-1 in murine macrophages. Free Radic Biol Med. 2017; 110:408–420. DOI: 10.1016/j.freeradbiomed.2017.06.014 [PubMed: 28690198]

[61]. Cadwell K, Stappenbeck TS, Virgin HW. Role of autophagy and autophagy genes in inflammatory bowel disease. Curr Top Microbiol Immunol. 2009; 335:141–167. DOI: 10.1007/978-3-642-00302-8_7 [PubMed: 19802564]

[62]. Fesus L, Demeny MA, Petrovski G. Autophagy shapes inflammation. Antioxid Redox Signal. 2011; 14:2233–2243. DOI: 10.1089/ars.2010.3485 [PubMed: 20812858]

[63]. Levine B, Mizushima N, Virgin HW. Autophagy in immunity and inflammation. Nature. 2011; 469:323–335. DOI: 10.1038/nature09782 [PubMed: 21248839]

[64]. Han QA, et al. Urolithin A attenuates ox-LDL-induced endothelial dysfunction partly by modulating microRNA-27 and ERK/PPAR-gamma pathway. Mol Nutr Food Res. 2016; 60:1933–1943. DOI: 10.1002/mnfr.201500827 [PubMed: 27060359]

[65]. Zhu G, et al. Geraniin attenuates LPS-induced acute lung injury via inhibiting NF-kappaB and activating Nrf2 signaling pathways. Oncotarget. 2017; 8:22835–22841. DOI: 10.18632/oncotarget.15227 [PubMed: 28423560]

[66]. Ip WKE, Hoshi N, Shouval DS, Snapper S, Medzhitov R. Anti-inflammatory effect of IL-10 mediated by metabolic reprogramming of macrophages. Science. 2017; 356:513–519. DOI: 10.1126/science.aal3535 [PubMed: 28473584]

[67]. Ko JH, Yoon SO, Lee HJ, Oh JY. Rapamycin regulates macrophage activation by inhibiting NLRP3 Inflammasome-p38 MAPK-NFkappaB pathways in autophagy- and p62-dependent manners. Oncotarget. 2017; 8:40817–40831. DOI: 10.18632/oncotarget.17256 [PubMed: 28489580]

[68]. Paschoal VA, et al. mTORC1 inhibition with rapamycin exacerbates adipose tissue inflammation in obese mice and dissociates macrophage phenotype from function. Immunobiology. 2017; 222:261–271. DOI: 10.1016/j.imbio.2016.09.014 [PubMed: 27692982]

[69]. Chimin P, et al. Adipocyte mTORC1 deficiency promotes adipose tissue inflammation and NLRP3 Inflammasome activation via oxidative stress and de novo ceramide synthesis. J Lipid Res. 2017; doi: 10.1194/jlr.M074518

[70]. Tang L, et al. Urolithin A alleviates myocardial ischemia/reperfusion injury via PI3K/Akt pathway. Biochem Biophys Res Commun. 2017; 486:774–780. DOI: 10.1016/j.bbrc.2017.03.119 [PubMed: 28343995]

[71]. Kosmala M, et al. Chemical composition of blackberry press cake, polyphenolic extract, and defatted seeds, and their effects on cecal fermentation, bacterial metabolites, and blood lipid profile in rats. J Agric Food Chem. 2017; 65:5470–5479. DOI: 10.1021/acs.jafc.7b01876 [PubMed: 28631469]

[72]. Fulda S. Autophagy in cancer therapy. Front Oncol. 2017; 7:128.doi: 10.3389/fonc.2017.00128 [PubMed: 28674677]

[73]. Bravo-San Pedro JM, Kroemer G, Galluzzi L. Autophagy and mitophagy in cardiovascular disease. Circ Res. 2017; 120:1812–1824. DOI: 10.1161/CIRCRESAHA.117.311082 [PubMed: 28546358]

[74]. Ueno T, Komatsu M. Autophagy in the liver: functions in health and disease. Nat Rev Gastroenterol Hepatol. 2017; 14:170–184. DOI: 10.1038/nrgastro.2016.185 [PubMed: 28053338]

[75]. Heilman J, Andreux P, Tran N, Rinsch C, Blanco-Bose W. Safety assessment of Urolithin A, a metabolite produced by the human gut microbiota upon dietary intake of plant derived ellagitannins and ellagic acid. Food Chem Toxicol. 2017; doi: 10.1016/j.fct.2017.07.050

[76]. Blander JM, Longman RS, Iliev ID, Sonnenberg GF, Artis D. Regulation of inflammation by microbiota interactions with the host. Nat Immunol. 2017; 18:851–860. DOI: 10.1038/ni.3780 [PubMed: 28722709]

Europe PMC Funders Author Manuscripts

Europe PMC Funders Author Manuscripts

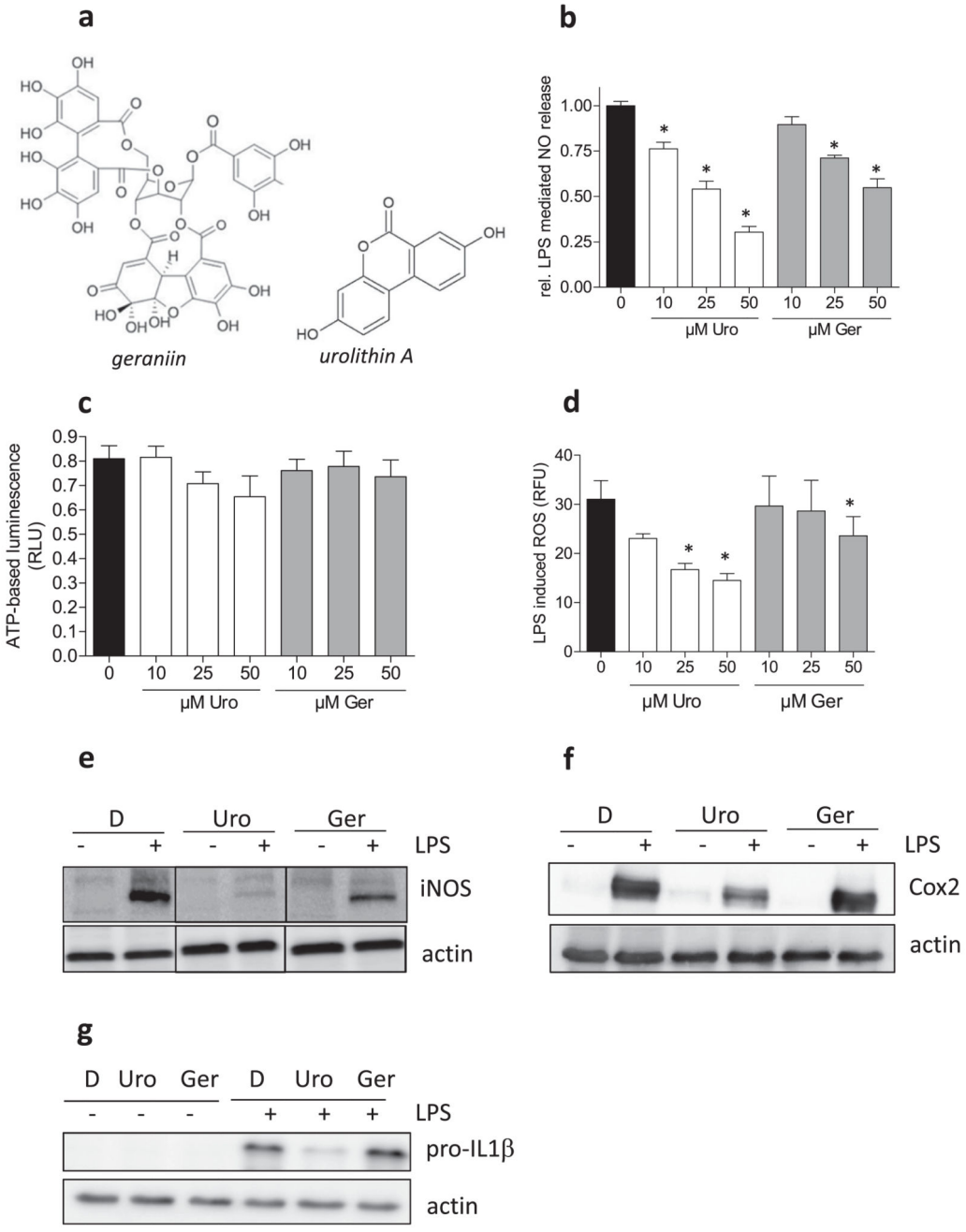

Fig. 1. Influence of geraniin and urolithin A on M1(LPS) macrophage polarization.

(a) Chemical structures of geraniin and urolithin A. (b) J774.1 macrophages were seeded in 96-well plates and treated with the indicated concentrations of urolithin A (Uro) or geraniin (Ger) in the absence and presence of 100 ng/mL LPS for 24 h. Supernatants were subjected to a Griess assay. The bar graph depicts data from three independent experiments in quadruplicates. Data are expressed as the LPS-triggered NO release (Δ +/−LPS of each condition) assessed by photometric readings at 550 nm (*, $p < 0.05$; *vs* DMSO control). (c) Attached cells in the plate were then subjected to a CellTiterGlo Cell viability assay. The

displayed data are the mean from three independent experiments and show viability of LPS-treated macrophages in the presence of the indicated concentrations of Uro and Ger (expressed as relative luminescence units (RLU)). (d) Macrophages were treated with Uro and Ger as well as LPS as indicated for 24 h before intracellular ROS levels were determined by flow cytometry. Compiled auto-fluorescence-corrected relative fluorescence units (RFU) of three independent experiments are shown (*, $p < 0.05$; *vs* DMSO control). (e) Macrophages were treated with DMSO (D), urolithin A (Uro, 40 μM), geraniin (Ger, 40 μM) and LPS (100 ng/mL) as indicated for 24 h before total cell lysates were subjected to western blot analysis for iNOS and actin. Lines between the lanes indicate that those parts changed order, but originate from the same original membrane. (f) Cells were treated as in (e), but lysates were probed for Cox2 and actin. (g) Macrophages were treated with D, Uro, Ger (each 40 μM) and LPS as indicated for 4 h before total cell lysates were subjected to western blot analysis for pro-IL-1β and actin. All shown blots are representative for three independent experiments for each target protein with consistent results.

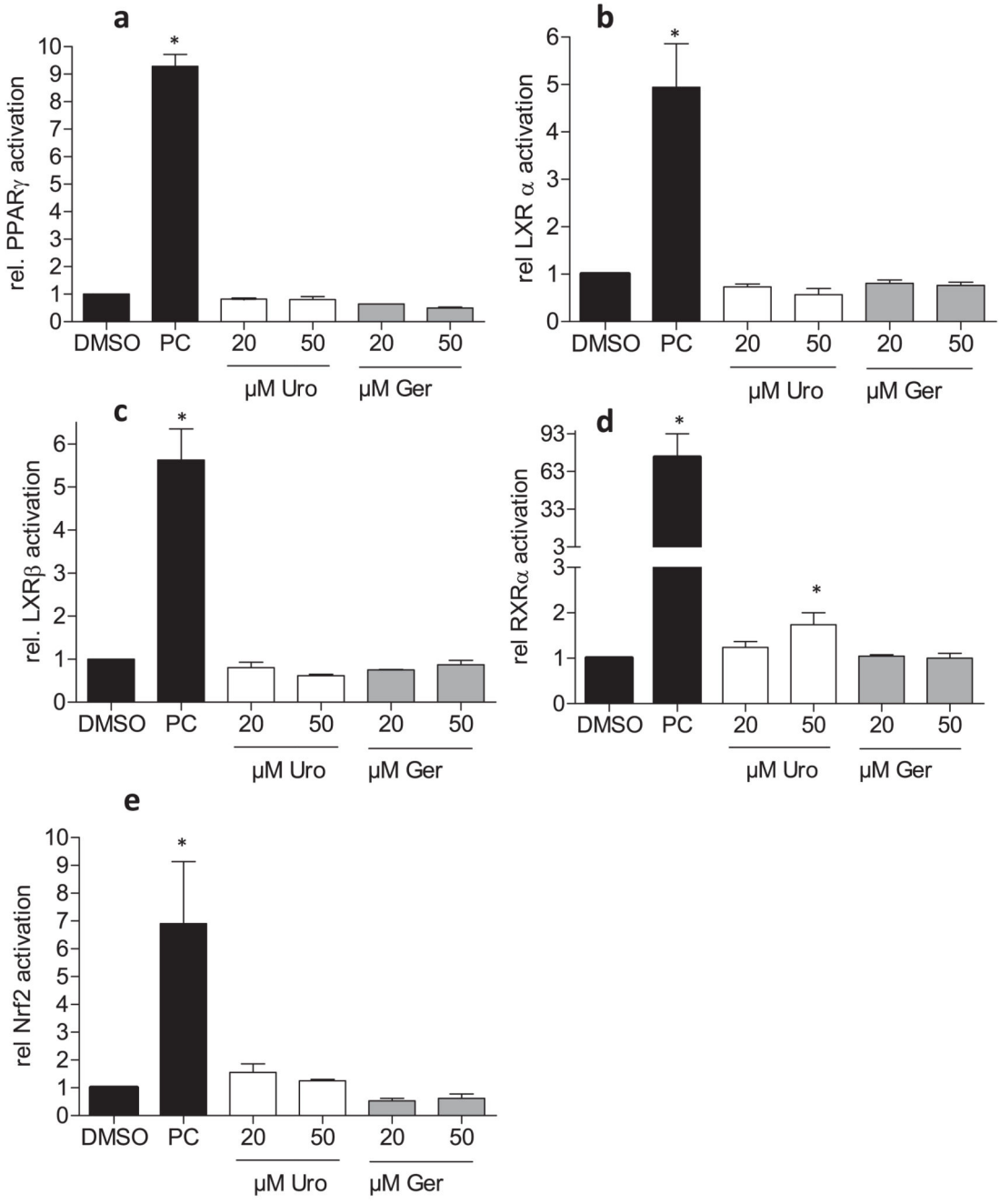

Fig. 2. Influence of geraniin and urolithin A on nuclear receptor- and Nrf2-dependent transactivation.

(a) HEK293 cells were transiently transfected with a PPARγ expression plasmid, a PPAR-dependent luciferase reporter (PPRE-LUC) construct as well as a plasmid coding for EGFP. Cells were seeded into 96–wells and treated with the indicated concentrations of Uro and Ger as well as 5 μM pioglitazone as positive control (PC) for 24 h. Then cells were lysed and luciferase-derived luminescence as well as EGFP fluorescence (control for cell number and transfection efficiency) were assessed. Data are expressed as the ratio between luminescence/fluorescence of each well and expressed as fold induction compared to the

solvent (DMSO) control. (n = 3) (b–d) HEK cells were treated basically as in (a), except for the use of LXRα- (b), LXRβ- (c) and RXRα (d) expression plasmids and the respective luciferase reporter constructs. 1 μM GW3965 and 5 μM retinoic acid served as positive controls (PC) for LXR α or β and RXRα, respectively. (e) Stably transfected CHO-ARE LUC/EGFP cells were seeded in 96-well plates and treated with the indicated concentrations of Uro and Ger as well as 100 nM CDDO-IM as positive control. After 16 h luminescence and fluorescence were recorded in the cell lysates. Data are expressed as the ratio between luminescence/fluorescence of each well and expressed as fold induction compared to the solvent (DMSO) control (n = 3) (*, $p < 0.05$; *vs* DMSO control).

Europe PMC Funders Author Manuscripts

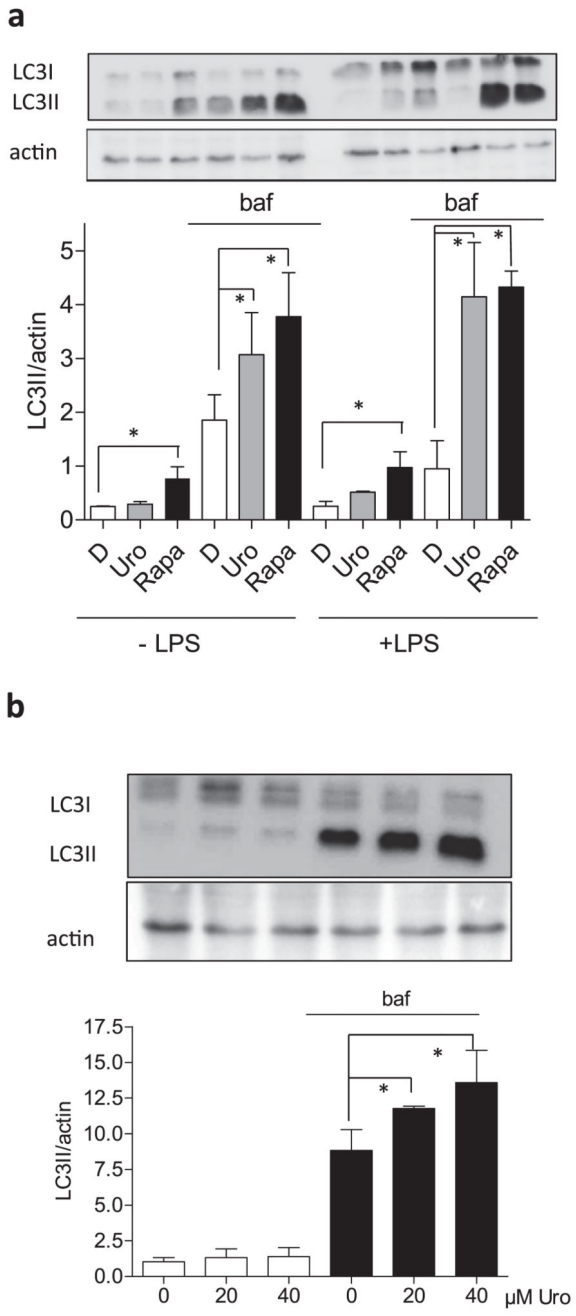

Fig. 3. Influence of urolithin A on the autophagic flux in macrophages.

(a) J774.1 cells were treated with 40 μM urolithin A (uro) and rapamycin (Rapa, 250 nM) for 24 h. As indicated, cells were additionally treated with 100 nM bafilomycin (baf) for the last 4 h. Cell lysates were prepared and subjected to western blot analysis for LC3 (I: non-lipidated, II: lipidated) as well as actin as loading control. Blots are representative for three independent experiments, and the bar graph compiles the densitometric data (LC3II/actin) from the three experiments. (b) J774.1 macrophages were treated with 0–40 μM urolithin A (uro) for 24 h and +/− bafilomycin (100 nM) for the last 4 h. Cell lysates were prepared and

treated as above. Again, representative blots as well as compiled densitometric data from three independent experiments are depicted (*, $p < 0.05$).

Europe PMC Funders Author Manuscripts

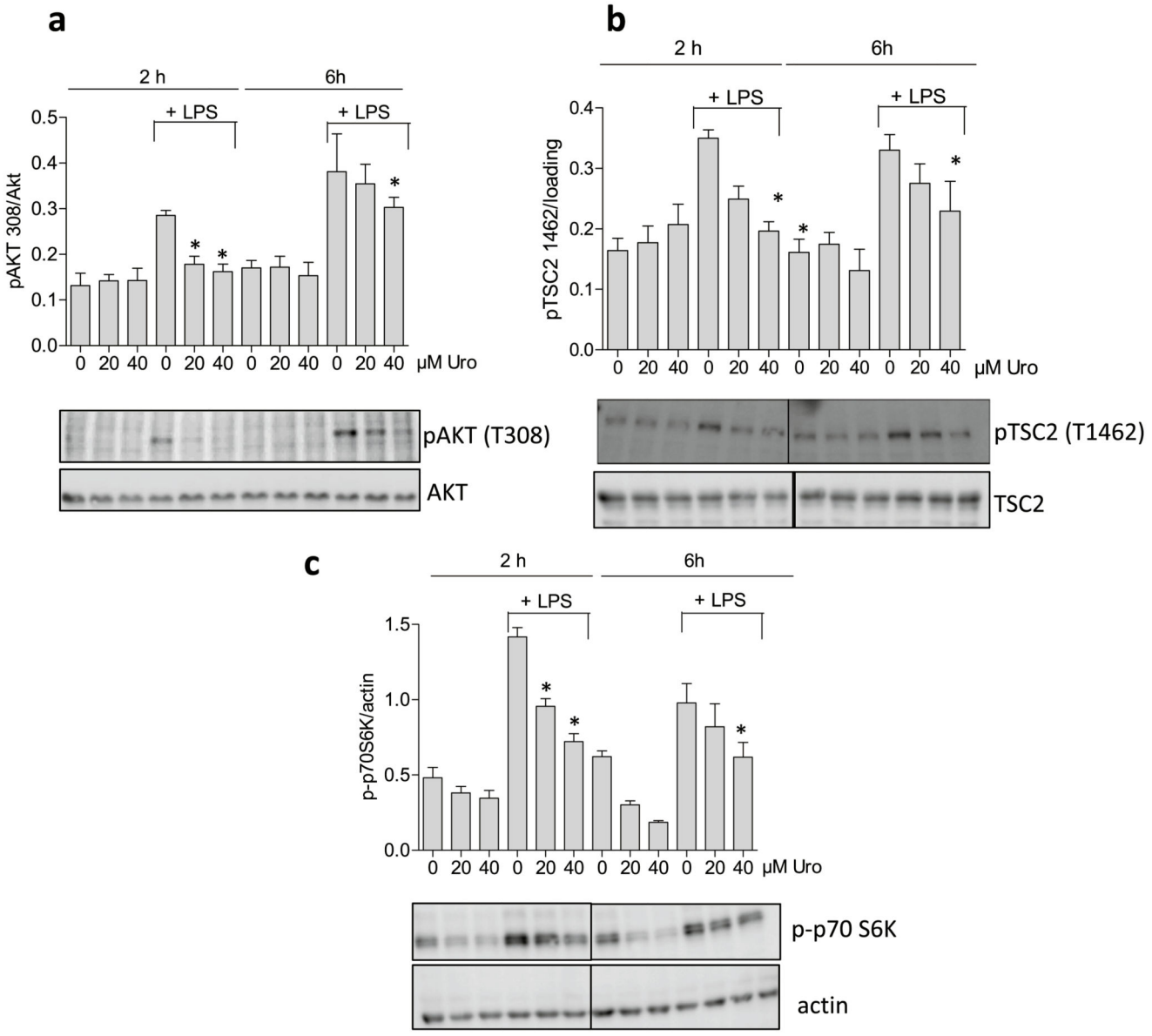

Fig. 4. Influence of urolithin A on the mTOR signaling pathway in macrophages.

Murine macrophages were treated with 20 and 40 μM urolithin A (Uro) in the presence and absence of LPS for 2 and 6 h. Cell lysates were prepared and subjected to western blot analysis for (a) phospho AKT (Thr308) and total AKT, for (b) phospho-TSC2 (Thr1462) and total TSC2, and (c) phospho-p70S6K (Ser389) and actin. Representative blots from three experiments and compiled densitometric data (target/loading control) are depicted (*, $p < 0.05$; *vs* LPS-treated solvent control).

Europe PMC Funders Author Manuscripts

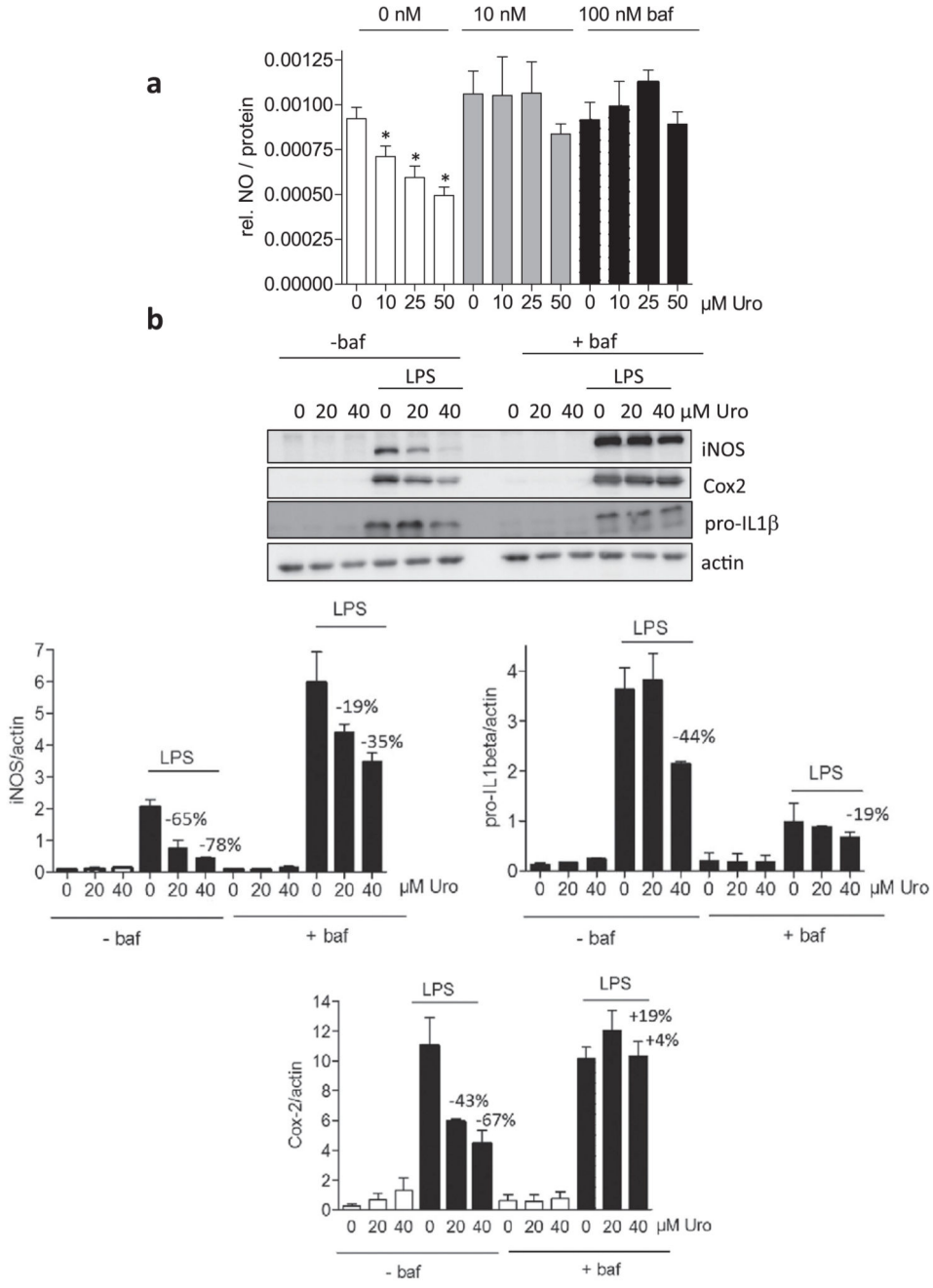

Fig. 5. Influence of an autophagy inhibitor on the reduced M1(LPS) polarization in the presence of urolithin A.

(a) J774.1 macrophages were treated with the indicated concentrations of urolithin A (Uro) in the absence and presence of 10 nM or 100 nM bafilomycin (baf) and then stimulated with 100 ng/mL LPS for 24 h. Supernatants were subjected to a Griess assay. The bar graph depicts data from three independent experiments in quadruplicates. Data are expressed as the LPS-triggered NO release (Δ +/−LPS of each condition) assessed by photometric readings at 550 nm. (*, $p < 0.05$; *vs* DMSO control) (b) J774.1 macrophages were treated with Urolithin A (20 and 40 μM), LPS (100 ng/mL) and bafilomycin (baf, 10 nM) as indicated for 4 (pro-

IL1 β) or 24 (iNOS, Cox2) hours. Total cell lysates were then subjected to western blot analysis for iNOS, Cox2, pro-IL1β and actin. Representative blots are depicted together with the compiled densitometric analysis of three independent experiments. The given numbers represent the % inhibition by urolithin A compared to the solvent (DMSO) control.

Europe PMC Funders Author Manuscripts

Europe PMC Funders Author Manuscripts

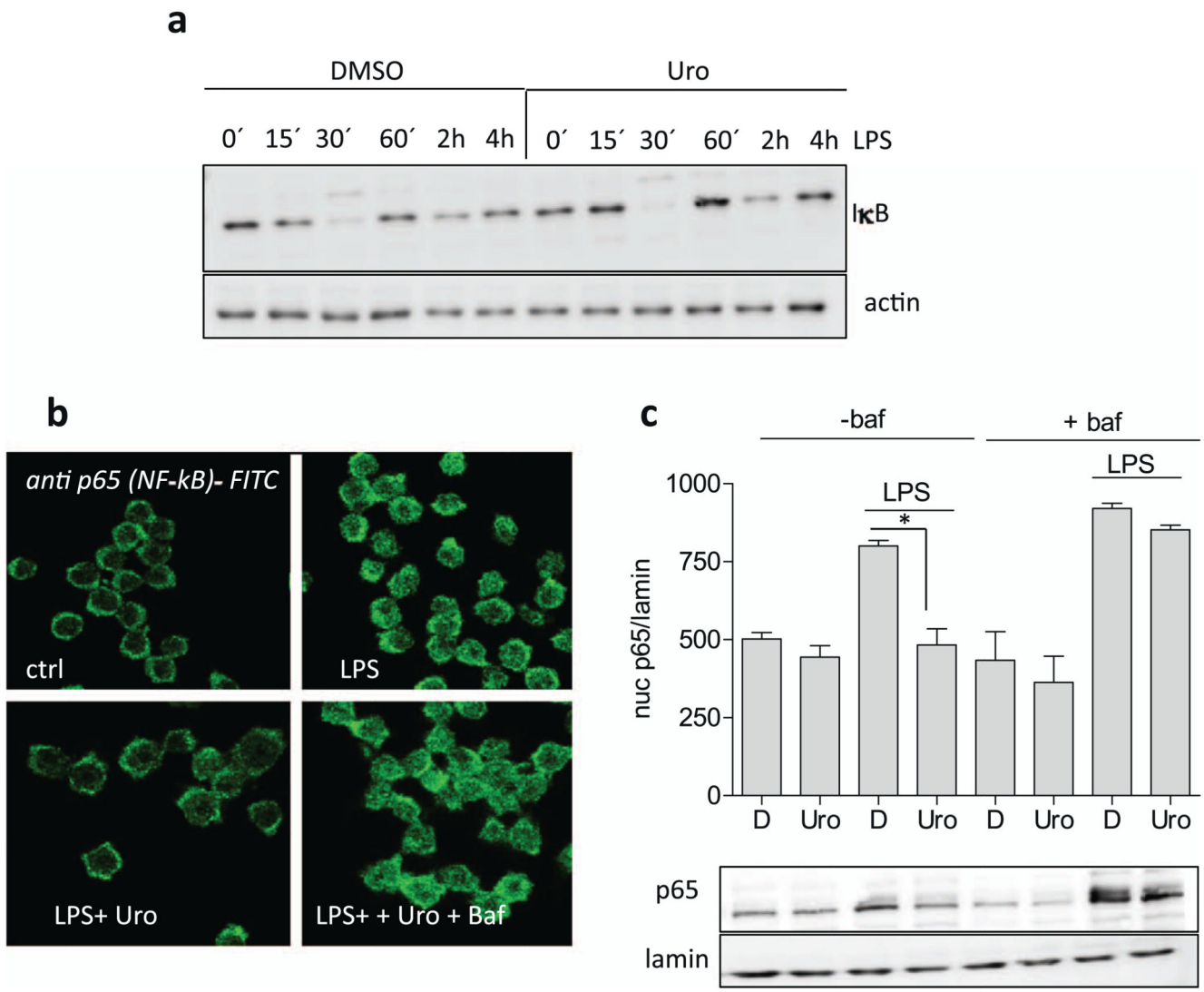

Fig. 6. Influence of urolithin A and/or autophagy inhibition on IκB degradation and nuclear translocation of p65.

(a) Murine macrophages were treated with solvent (DMSO) or 40 μM urolithin A (Uro) and then stimulated with LPS (100 ng/mL) for the indicated periods of time. Total cell lysates were then subjected to immunoblot analysis for IκB and actin. Representative blots from three independent experiments are depicted. (b) J774.1 cells were grown on coverslips and then treated with urolithin A (Uro, 40 μM), LPS (100 ng/mL) and bafilomycin (100 nM; baf) as indicated for 1 h. Then immunostaining for p65 was performed and cells were viewed under a confocal microscope. (c) J774.1 cells treated with urolithin A (Uro, 40 μM), LPS (100 ng/mL) and bafilomycin (100 nM; baf) as indicated for 1 h. Then nuclear protein was isolated and subjected to western blot analysis for p65 and lamin B. Representative blots and compiled densitometric data from three independent experiments are depicted. (*, $p < 0.05$)